IEEE Access
Multidisciplinary | Rapid Review | Open Access Journal

Received January 8, 2021, accepted February 11, 2021, date of publication February 24, 2021, date of current version March 4, 2021.

Digital Object Identifier 10.1109/ACCESS.2021.3061669

Application Study of a New Underwater Glider With Single Vector Hydrophone for Target Direction Finding

CHAO WANG AND MENG YUAN
Navy Submarine Academy, Qingdao 266199, China
Pilot National Laboratory for Marine Science and Technology, Qingdao 266237, China

Corresponding author: Meng Yuan (yuanm2012@foxmail.com)

This work was supported by the National High Technology Research and Development Program of China under Grant 2019YFC0311700.

ABSTRACT The underwater glider is propelled by changing the buoyance of itself and glides forwards with the help of the hydrodynamic force. It enables the people to conduct large-scale and long-term marine observation and detection with good stealthiness, thus, it plays an important role in the stereoscopic observation system of the transparent marine engineering. Integrated with a single vector hydrophone, the underwater glider platform can perform a full-space and unambiguous direction-finding of the underwater target. Moreover, the transient and strong noise interference of platforms, produced by buoyance adjustment, pitch adjustment and propeller rotation of the glider, can be avoided by controlling the working time of the acoustic system. As for the strong and intermittent electromagnetic brake interference produced by the heading regulating mechanism, its influence on the acoustic system can be reduced or even eliminated by the vibration and noise reduction technique. To verify the target detection estimation performance of the underwater glider (before and after the vibration and noise reduction processing), pre- and post-experiments are conducted in the South China Sea in May 2018 and August 2019, respectively. The results show that before the vibration and noise reduction, interfered by the intermittent electromagnetic brake noise, the farthest detection distance of the underwater glider to the experimental ship with the velocity of 10 kn is only approximately 5 km. After the optimization, the farthest detection distance of the underwater glider to the experimental ship with the velocity of 8.4 kn can reach to 7.7 km and without the influence of the intermittent noise interference of the platform.

INDEX TERMS Underwater glider, vector hydrophone, vibration and noise reduction, target direction estimation, South China Sea.

I. INTRODUCTION

As a new type of unmanned moving observational platform, the underwater glider is an underwater submerged equipment with advantages of long operation time, far sustainable range, low noise level, good stealthiness, low cost and easy operation, and is widely applied in the field of the marine ambient observation. Compared with the traditional observation methods such as buoys, subsurface buoys, the application of the underwater glider in the marine ambient observation has more obvious advantages [1]–[7]. The underwater glider only produces transient and predictable platform noises at the stage of diving from the water surface, controlling the heading, surfacing at the maximum working depth or starting the propeller under emergent situations. Therefore, the underwater glider platform can be integrated with the acoustic system, and the influence of the platform noises on the acoustic system can be avoided and reduced by controlling the working time of the acoustic system and conducting the vibration and noise reduction to the glider platform [8]–[10].

In recent years, the application of the underwater glider on the acoustic monitoring has been paid much attention with the development of the platform, sensor technology and acoustic signal processing [11]–[14]. The underwater glider integrated with the acoustic system started abroad at earlier time and made bigger progress. Seaglider extended a long pole at the tail of the platform and was integrated with a hydrophone at the top of the pole. In 2006, a sea experiment was conducted

The associate editor coordinating the review of this manuscript and approving it for publication was Manuel Rosa-Zurera.

with 40 days sailing and 200 km of the voyage, which achieved a better effect. In 2006, the winged underwater acoustic gliders (Xray and ZRay) which were designed under the cooperation of American Scripps Maritime Research Institute and University of Washington, were equipped with the acoustic sensor related with the tactics in the wing. The acoustic sensor was used for cruising and detecting the silent-type targets in the ocean. In May of 2010, Slocum loaded with a hydrophone was laid out at the North of Lau Basin to detect the underwater volcano in West Mata. It recorded the variation of the sound wave amplitude with distance, and proved that the geology change could make the noise level of this area increase [12]. The experimental results showed that the glider could be effectively applied for the underwater acoustic detection. In May of 2013, Slocum loaded with SR-1 hydrophone, was used for detecting the underwater noise in Algarve University of Portugal. The result showed that it could conduct the effective detection for the underwater noise from the time and spatial dimension [14].

Researches on the integration of the underwater glider with the acoustic hydrophone are relatively few in China. In the Institute of Acoustics at the Chinese Academy of Sciences, the underwater glider integrated with single acoustic pressure hydrophone was used for conducting the observation test of the marine ambient noise in the waters of the South China Sea, in August of 2016. Due to the uncompleted platform optimization, the noise spectrum levels of the marine ambient at the high frequent bands of 800Hz and1.6 kHz were bigger than those at the low frequency band of 100 Hz and 200 Hz [9]. In Harbin Engineering University, the acoustic pressure hydrophone was equipped respectively at the left wing, right wing, front dome and tail wing, which constituted a quaternary acoustic detection system. A sea experiment has been done with it in the South China Sea, but the result only verified that the acoustic system had better gain for the single frequency signal. In Zhejiang University, the self-contained hydrophone was equipped respectively at the front and the trail of the glider forming a simple array with a large aperture, which was tested at sea twice, in Mariana Trench and South China Sea in April and August of 2018, respectively. Sea trials verified that the underwater glider had advantages in the marine ambient noise observation and target signal detection, but the results did not further verify the detection performance of the acoustic detection system to the moving targets at sea [15].

In this study, by integrating a single vector hydrophone on the head of an existing "Petrel-II" underwater platform of Tianjin University, a new type of underwater glider platform is developed with the function of target detection, which is shown in the Fig. 1. The vector hydrophone can synchronously and concurrently output the acoustic pressure scalar and particle vibration velocity or the orthogonal vector of particle vibration accelerated velocity, which makes the vector hydrophone with the unique advantage in the field of the acoustic detection [16]–[19]. For the intermittent electromagnetic brake noise interference of the platform during the working period of the heading regulating, the heading regulating mechanism and the heading regulating control strategy of the underwater glider are conducted with the vibration and noise reduction and the optimization. Two experiments are organized in the South China Sea in May of 2018 and August of 2019 to verify the target detection estimation performance of the underwater glider, and these experimental data are analyzed to compare the performance of the glider platform in detecting surface ships before and after the vibration and noise reduction processing.

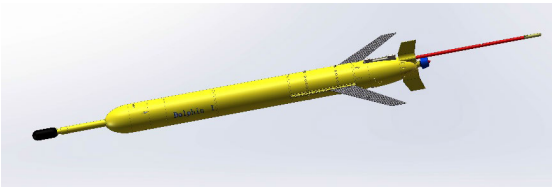

FIGURE 1. The diagram of the underwater glider loaded with a vector hydrophone.

II. ACOUSTIC MEASURING SYSTEM

The acoustic measuring system of the underwater glider is mainly composed of a single vector hydrophone and a four-channel signal processor. The adopted vector hydrophone is a co-vibrating vector hydrophone with the advantages of high sensibility, good directivity and high-resolution, and has been widely applied in the engineering project at present. The underwater glider platform integrated with a single vector hydrophone enables people toconduct the full-space, unambiguity, underwarter target direction finding, which provides spatial advantages for underwater small platforms loaded with acoustic sensors to conduct targets detection [20].

Fig. 2 shows the real photo of the underwater glider acoustic measuring system, in which the vector hydrophone is an irregular cylinder with hemisphere caps at both ends, and eight suspension holes are symmetrically distributed on the top and bottom end of hemisphere caps. The working frequency band is 20 Hz to 5 kHz and the weight in the air is about 450 g. The boundary dimension is φ66mm $\times$ 78 mm, and the maximum pressure-resistant depth is 1200 m. Sensibility of the vector hydrophone acoustic pressure channel does not change with the frequency, and the sensibility ≥ -192 dB (0 dB $=$ 1 V/μPa) in the whole range of tested frequencies. The sensibility of the vector channel changes with frequencies, specifically, the lower the frequency is, the smaller the sensibility is. The sensibility level of the vector channel is approximately -180 dB (0 dB $=$ 1 V/μPa) at the frequency point of 1 kHz [21]–[23]. The main tasks of the four-channel signal processor are to collect, store and process the signal received by the vector hydrophone. The four-channel signal processor adopts the design of DSP+FPGA with the total power dissipation 9 W and the capacity 256 GB. The four-channel signal processor consists of a power board, a simulation board, a digital board, and an upper computer. The processor also includes four RS232 interfaces and the

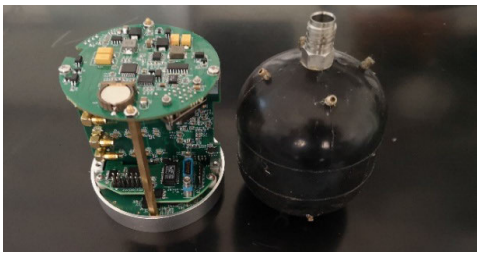

FIGURE 2. The real photo of the acoustic measuring system.

Internet access to transmit the information. The Internet access is mainly used for connecting the signal processor and the upper computer. When the upper computer is linked with the signal processor, it can be conducted with the operations of time service, formatting, data downloading and program updating.

III. NOISE ANALYSIS AND OPTIMIZATION OF THE UNDERWATER GLIDER PLATFORM

When the underwater glider performs underwater target detection tasks, it mainly adopts the working mode of profile gliding. During the working stage of the glider profile gliding, noises come from the attitude regulating unit and the buoyance regulating unit, and the attitude regulating unit includes the pitch regulating mechanism and the heading regulating mechanism. The pitch regulating mechanism adjusts the pitch angle by moving the battery pack forwards and backwards along with the platform principal axis to make the platform float up or dive down. Meanwhile, the heading regulating mechanism adjusts the roll angle by rotating the battery pack around the principal axis of the platform to control the heading when the glider deviates the planned course. When the glider dives to the maximum working depth, the oil pump motor starts to work and drains the hydraulic oil into the oil bag to increase the buoyance of the glider platform, which makes it complete the transitional control from diving to surfacing. The platform noise produced during the above process will significantly affect the underwater target direction-finding performance of the vector hydrophone.

During the process of profile gliding, the pitch regulating mechanism and the buoyance regulating unit only work when the glider is ready to dive on surface or the glider is ready to surface at the maximum depth. However, the heading regulating mechanism needs to work all the time to adjust its heading of the glider in real time. When the glider is ready to dive at the surface or to surface at the maximum depth, the acoustic measuring system is outage to stop working, namely, the platform noise produced by the pitch regulating mechanism and the buoyance regulating unit can be avoided. Therefore, it is especially required to analyze and optimize the platform noise produced by the glider heading regulating mechanism [8], [9].

The heading regulating mechanism of the glider Petrel-II achieves the self-locking of the rotation mechanism by the electromagnetic brake to adjust its roll angle, which makes it complete the heading control. However, the startup and shutdown of the electromagnetic brake will make the mechanism produce a strong impulse excitation and thus, cause strong vibration noise. Therefore, it is required to conduct the vibration and noise reduction process of the glider heading regulating mechanism and optimize the control strategy of the heading regulating mechanism to reduce the self-noise level. The vibration and noise reduction and the optimization of the glider course heading regulating mechanism are conducted from the following four aspects in this article.

A. INTENSITY REDUCTION OF THE VIBRATION SOURCE

1) STEERING REGULATING MECHANISM OPTIMIZATION METHOD

The original glider used for the marine ambient observationdrives the eccentric weight by the motor and gear drive mechanism to realize the heading control. The electromagnetic brake makes the heading mechanism self-locking, and the brake switch produces the stronger impulse excitation on the mechanism to cause the vibration noise of the shell. Gear drive mechanism produces the interdigitation noise during the interdigitation. The drive motor adopts Hall sensor to conduct the electronic commutation with about 14% torque fluctuation. All noises above can interfere the signal-receiving of the acoustic system seriously. In order to avoid the vibration noise produced by the electromagnetic brake, reduce the interdigitation noise of the gear, and eliminate the torque noise of the drive motor, the worm gear with the function of the self-locking is adopted to adjust the roll angle of the glider, which can avoid the noise of the electromagnetic brake. Moreover, the interdigitation of the worm gear is stable and can reduce the interdigitation noise of the gear. An encoder is added on the drive motor of the roll mechanism to improve the control accuracy of the motor rotation, thereby eliminating the torque fluctuation and improving the rotation stability of the rolling weight. These optimization designs of the heading regulating mechanism above will reduce the self-noise of the heading regulating mechanism of the glider, thereby reducing the interference influence of the heading regulating mechanism on the acoustic system.

2) STEERING CONTROL OPTIMIZATION STRATEGY

To ensure the stability of the revolution speed of the underwater glider steering regulating mechanism, the driving motor adopts the speed closed-loop control and uses the proportional-integral-derivative (PID) algorithm to adjust the revolution speed. However, when the eccentric weight rotates, the load changes and makes the revolution speed of the motor fluctuate. For example, if the PID parameters are not appropriate, they will increase the vibration, or even cause the vibration divergence. Thus, the PID parameters should be optimized according to the special conditions of the driving motor load changes, and the optimal PID parameters should be chosen to improve the rotation stability of the steering regulating mechanism to reduce the vibration noise. In addition,

the revolution speed of the motor should be set reasonably according to the requirements of the glider status. This way can make the frequency of the noise that produced by the roll mechanism far away from the frequency that observed from the marine ambient noise and avoid the bad influence of the roll mechanism on the acoustic system.

B. VIBRATION FREQUENCY DESIGN OF THE HEADING REGULATING MECHANISM

When the heading regulating mechanism of the underwater glider is working, the noise frequency produced mainly depends on the structure, the material and the motor rotational speed of the heading regulating mechanism. On basis of the modal analysis of the structure, the structure design of the heading regulating mechanism is optimized, and the rotational speed of the motor is reasonably set according to the performance requirement of the glider to make the noise frequency produced by the rolling mechanism far way form the detection range of the acoustic system and avoid the bad influence of the noise on the detection performance of the acoustic system.

C. WAYS TO BLOCK NOISE TRANSMISSION

There are two main ways for the glider platform vibration noise to affect the acoustic system, which are the conduction propagation of the structure and the spatial radiation propagation. For the conduction propagation, a damping structure is designed among the acoustic load, the steering regulating mechanism and the glider shell to cut off the transmission route of the vibration noise from the steering regulating mechanism to the acoustic load. For the spatial radiation propagation, the noise can be reduced by painting rubber sound-absorption material inside of the glider shell and arranging sound-absorption modules inside of the glider.

D. OPTIMIZATION DESIGN OF THE ELETROMAGNETIC COMPATIBILITY

The heading regulating mechanism of the underwater glider is a variable load which can cause the current fluctuation of the drive motor andfurther affect the power supply stability of the dry-end circuit of the glider, which will cause the bad influence on the acoustic system. To ensure the stability of the acoustic system under working condition, the optimization design of the electromagnetic compatibility is conducted on the existing underwater glider platform. An independent pressure cabin is designed. The electromagnetic radiated interference is shielded. The independent isolated power supply is adopted to block the electromagnetic conduction interference.

Fig. 3 and Fig. 4 show the time-domain noise waveform collected by the acoustic pressure channel of the vector hydrophone and the frequency spectrum diagram obtained by the heading regulating mechanism during its working period. The images on the left belong to the original signal while the images on the right have been processed by the vibration and noise reduction technique. It can be seen that the heading

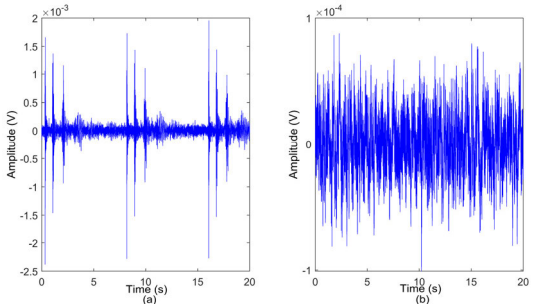

FIGURE 3. The time-domain signal received by the acoustic pressure channel of the vector hydrophone when the glider adjusts the heading. (a) Before the vibration and noise reduction and (b) after the vibration and noise reduction.

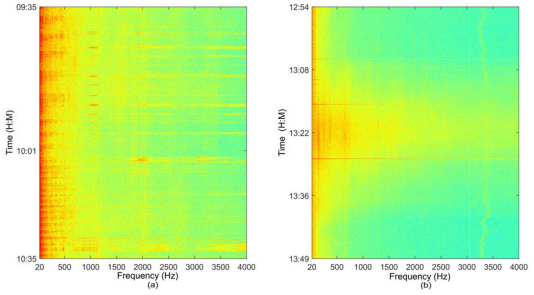

FIGURE 4. Frequency spectrum diagram of the signal received by acoustic pressure channels of the vector hydrophone. (a) Before the platform optimization and (b) after the platform optimization.

regulating mechanism produces strong intermittent electromagnetic brake interference impulse signal, but the impulse interference can be eliminated after the optimization of the vibration and noise reduction. We quantitatively compared the changes in the noise spectrum level of each channel of the vector hydrophone during the working period of the glider heading adjustment mechanism before and after the optimization of vibration and noise reduction (Fig. 5). It can be seen that: (1) After the optimization, the noise interference produced by the heading adjustment mechanism on the vector hydrophone is greatly reduced. Among them, the noise of the vector hydrophone's sound pressure channel at 2 kHz frequency is reduced by a maximum of 25 dB, and the noise at 80Hz frequency is reduced by a maximum of 28 dB. (2) After the optimization, the noise spectrum levels of the vector hydrophone acoustic pressure channel are always smaller than those of the marine ambient noise under the sea state of level 0 in the entire frequency range; However, the noise spectrum levels of the vector hydrophone vector channels are still higher than the marine ambient noise under the sea state of level 6 in the range of the low frequency bands that below 200 Hz. This is because the sensibility of the vector channels is lower at low frequency bands and they are more sensitive to the vibration noise of the platform.

IV. TARGET BEARING ESTIMATION

A. MINIATURE ATTITUDE SENSOR

When underwater swaying platforms, such as the underwater glider, buoy and subsurface buoy loaded with vector

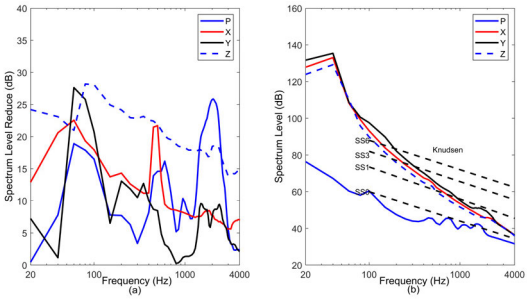

FIGURE 5. (a) Noise reduction spectrum levels with the optimization of the glider platform and (b) self-noise spectrum levels with the optimization of the glider platform.

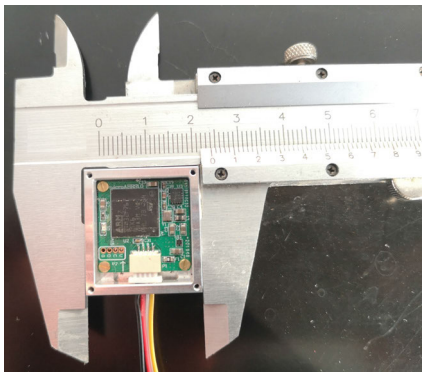

FIGURE 6. The real picture of the micro-attitude sensor.

hydrophones, conduct underwater target detection, the vector hydrophone will bring attitude changes in terms of pitch, reversal and roll. The target bearing detected by the vector hydrophone is based on its own coordinate system. However, in order to obtain the target bearing relative to the geographic coordinate system, it is necessary to provide the real-time attitude information of the vector hydrophone relative to the geographic coordinate system, and then the accurate target bearing can be obtained by the attitude correction. In this study, a micro-electro-mechanical system (MEMS) attitude sensor is integrated in the pressure tank of the glider platform acoustic system, which is used to measure the heading, pitch, and roll angles of the vector hydrophone (Fig. 6). The heading angle 0° represents the head of the glider facing due north, and the heading angle will change from 0° to 360° if the glider turns one circle clockwise. The roll angle 0° indicates that the glider wing is horizontal, and the roll angle to the left is positive while to the right is negative (looking from the tail of the glider towards the head). The range of roll angle is ±180°. A pitch angle 0° indicates that the glider is horizontal. The pitch angle should be positive when the glider attitude is downward, and the pitch angle should be negative when the attitude is upward. The range of pitch angle is ±90°.

Micro-attitude sensor is mainly composed of sensor module and computer control module. The sensor module is composed of triaxial MEMS gyroscope, triaxial MEMS accelerometer and triaxial MEMS magnetometer, which are used for measuring components at three quadrature axis of the angular velocity, accelerated velocity of the platform,

TABLE 1. Accuracy testing results of the heading angle at the dynamic state.

Frequency (Hz)	Standard amplitude (°)	Measured amplitude (°)	Error (°)
0.1	19.76	19.3	0.46
0.3	15.48	15.1	0.38
0.5	19.36	19.0	-0.36
0.7	15.16	14.8	-0.36
0.9	7.47	7.3	-0.17
1	6.82	6.7	-0.12
2	3.63	3.5	-0.13

and the intensity of the geomagnetic field of its environment, respectively. They are connected together to measure the coordinate system mutually overlapping. The test result shows that the micro-attitude sensor can resolve the attitude with the maximum speed of 540 Hz and output the attitude angle with the speed of 20 Hz or higher speed by serial port RS232 bus.

The performance parameters of the micro-attitude sensor are tested in the First Measurement and Testing Research Center of Science and Technology Industry of National Defense. The testing projects include the accuracy test of the heading angle, pitch angle and roll angle at the static state and dynamic state. The accuracy tests at the static state show that the maximum error values of the heading angle, pitch angle and roll angle at the static state are respectively 0.8°, 0.1° and 0.2°. The accuracy tests at the dynamic state respectively measure the accuracy at the dynamic state at seven frequencies of 0.1 Hz, 0.3 Hz, 0.5 Hz, 0.7 Hz, 0.9 Hz, 1 Hz and 2Hz on the direction of three axis. The test results show that the error values of the heading angle, pitch angle and roll angle at the dynamic state are respectively less than or equal to 0.5°, 0.4° and 0.5°, when the vibration amplitude is less than 20° and the frequency is less than 2 Hz. In the following table, the accuracy testing results of the heading angle at the dynamic state are shown, which can be seen that the micro-attitude sensor has better measurement accuracy of the attitude angle.

B. ATTITUDE CORRECTION

Mark the Cartesian coordinate system as $Ox_by_bz_b$, which is used for the vector hydrophone to measure the particle vibration. Mark the geographic coordinate system applied by the attitude sensor as $Ox_ny_nz_n$. The Ox_n, Oy_n, and Oz_n axis of the geographic coordinate system point to the north, the east, and the sky, respectively. When the coordinate system $Ox_by_bz_b$ rotates relative to the coordinate system $Ox_ny_nz_n$, the variation in Oz_n axis is heading angle α, the variation in Ox_n axis is pitch angle β, and the variation in Oy_n axis is roll angle γ (Fig. 7).

Supposed (x_b, y_b, z_b) is the coordinate value of the coordinate system $Ox_by_bz_b$, and (x_n, y_n, z_n) is the coordinate value of the geographic coordinate system $Ox_ny_nz_n$, the mapping relationship between the two coordinate values can be

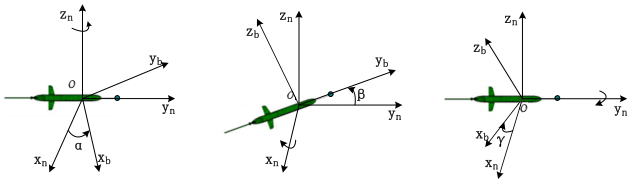

FIGURE 7. Schematic diagram of the attitude angle definition.

obtained by the attitude transition matrix as follows:

$$(x_n, y_n, z_n)^T = C_b^n \cdot (x_b, y_b, z_b)^T$$

where C_b^n denotes the attitude transfer matrix, and its expression is presented as shown at the bottom of the page.

C. DIRECTION-FINDING METHOD BY A SINGLE VECTOR HYDROPHONE

There are many target bearing estimation algorithms based on single vector hydrophone. Generally, they can be divided into two categories according to the direction-finding principle. One kind is based on the bearing estimation of the acoustic energy flow, such as the acoustic intensity average, the cross-spectrum method, the histogram method, the weighted histogram method, and so on; The other kind considers the various channels of the vector hydrophone as multivariate arrays, in which each array element is at the same point of the space. Since the vector hydrophone itself conforms to the characteristics of the array flow pattern, the existing array signal processing methods can be applied to the single vector hydrophone.

The windowing histogram bearing estimation method is used in the current study, which is more adapted to the engineering application with better robustness and stability. The windowing histogram bearing estimation method is a statistic method based on the complex sound intensity, namely, each frequency point within the processed frequency bands is conducted with the bearing estimation on basis of the conjugate cross spectrum between the acoustic pressure and the particle vibration velocity. The omnidirectional 360° is divided into bearing intervals every 1° or 0.5°. Counting the number of frequency points within each bearing interval and the bearing corresponding to the maximum number are regarded as the target estimation bearing. This is called the histogram statistical method. In practical applications, in order to increase the detection ability of the vector hydrophone, people need to improve the processing gain by time accumulation, namely, time windowing. However, the accumulation time should neither be too long nor too short. If the accumulation time is too long, it may cause a large bearing estimation deviation for targets with fast bearing change rate, and if the accumulation

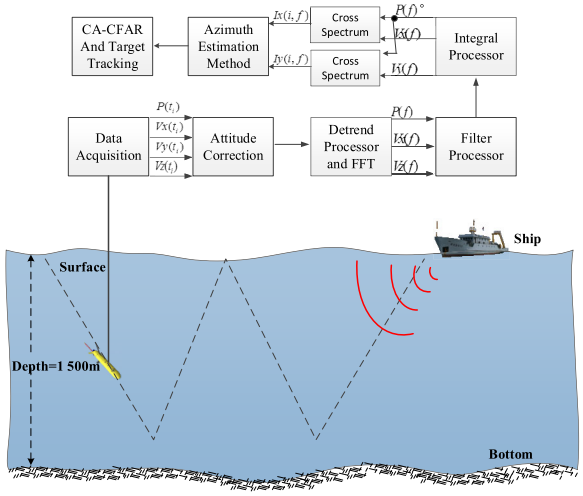

FIGURE 8. The bearing estimation flow chart of windowing histogram method.

time is too short, the gain would be too small. In this study, a 5s-time-window is adopted to process the data with the processing frequency band of 200 Hz∼3 kHz. The fast-Fourier-transform (FFT) time length of each calculation is 1 s while the FFT step pitch is 0.25 s. Thus, seventeen groups of acoustic intensity flow spectrum are obtained within each time window. After the average, the histogram statistical method can be used to conduct the bearing estimation, and this processing method by time windowing is called the windowing histogram method. During target direction-finding process, the false alarm probability of target detection can be kept constant by the cell-averaging constant false alarm rate (CA-CFAR) processors, and then the target bearing tracking can be realized. The whole calculation process of the method is shown in Fig. 8.

In Fig. 8, $i = 1, \cdots, 17$, the function of the detrending processor is to detrend low-frequency trend items of the acoustic signal received by the vector hydrophone. The calculation formula of the target bearing is presented as follows:

$$\theta(f) = arc\tan\frac{\mathrm{Re}\langle Pw^*(f) * Vyw(f)\rangle}{\mathrm{Re}\langle Pw^*(f) * Vxw(f)\rangle} = arc\tan\frac{\langle Iy(i,f)\rangle}{\langle Ix(i,f)\rangle}$$

It can be seen from the above formula that the target bearing, which is calculated by the above formula, is related to the frequency f. The estimation values of the target bearing are not the same among different frequency points. The narrowband interference and strong line spectrum interference existing in the environment can be restrained with the windowing histogram method. However, when there are multiple targets in the environment or the frequencies of the radiated noise are mutually overlapping, this method can only obtain the

$$C_b^n = \begin{bmatrix} \cos\gamma\cos\alpha - \sin\gamma\sin\beta\sin\alpha & -\cos\beta\sin\alpha & \sin\gamma\cos\alpha + \cos\gamma\sin\beta\sin\alpha \\ \cos\gamma\sin\alpha + \sin\gamma\sin\beta\cos\alpha & \cos\beta\cos\alpha & \sin\gamma\sin\alpha - \cos\gamma\sin\beta\cos\alpha \\ -\sin\gamma\cos\beta & \sin\beta & \cos\gamma\cos\beta \end{bmatrix}$$

compound bearing of the acoustic energy flow of each target, resulting in a large deviation from the true bearing. The purpose of histogram bearing statistics is to count the target estimation bearing $\theta(f)$ in corresponding bearing intervals according to frequency points. Supposed each bearing interval is 1°, then the following is derived:

$$k = [\theta(f) * 180/\pi]$$
$$\varphi(k) = \varphi(k) + 1$$

In the above formula, the square bracket [ ] expresses rounding operation, if $\theta(f) \leq 0$, then $\theta(f) = \theta(f) + 360$, the target estimation bearing is located within the range of [1 360]. φ is the frequency of the bearing estimation at each angle, and the angle value corresponding to the maximum value is the target estimation bearing.

V. EXPERIMENTAL DATA ANALYSIS

A. EXPERIMENT DESCRIPTION

Since 2013, integrated with the vector hydrophone, the ''Petrel-II'' underwater glider platform has conducted several experiments both in the anechoic tank and in the ocean. Two experiments were organized in the South China Sea in May of 2018 and August of 2019 to verify the target detection estimation performance of the underwater glider. Experimental data were used to compare the performance of the glider platform in detecting surface ships before and after the vibration and noise reduction processing. The glider adopts the working mode of profile gliding during the experiments under the sea state of level 2, and the spectrum level of the marine ambient noise was 54 dB@1kHz. During these experiments, results of the acoustic velocity profile measured by the conductivity-temperature-depth (CTD) system show that there was a homogeneous layer within the sea depth of 30 m. The acoustic channel axis was near the depth of 1000 m, and the seabed in experimental area was flat and sandy.

B. EXPERIMENT ORGANIZED IN MAY of 2018

To verify the detection performance of the new-type glider on the surface targets under deep sea conditions, an experimental ship (length 40 m, width 8 m) was used as the detection target, and the detection ability verification test of the underwater glider was firstly carried out in the South sea in May of 2018. The maximum diving depth of the glider was set to 400 m. Fig. 9(a) and (b) indicates the depth changes of the platform and the variation of the attitude angle with time during the process of underwater glider profile gliding in experiments. It can be seen that: firstly, during the period of profile gliding from 09:35 to 10:35, the maximum diving depth of the underwater glider platform is 360 m and the profile duration is approximately 1h. The acoustic system is on electricity to collect signals at 09:35. When the glider drains oil and adjusts the attitude and buoyance, the acoustic system is outage to stop working approximately for fifteen minutes from 10:01 to 10:15, and then the acoustic system is on electricity to work again at 10:15. The underwater glider floats to surface and the acoustic system is outage to stop working at 10:35. The working duration of the acoustic system is forty-five minute in the whole profile process. Secondly, the roll angle of the glider is continuously adjusted to control the heading of the glider platform during the process of profile gliding. The heading angle changes greatly when the glider is ready to dive from the surface or ready to drain oil to surface. During the process of profile gliding, the fluctuation of the heading angle is within 35°. In addition, the pitch angle only changes when the glider platform is in the maximum diving depth. The pitch angle of the glider is approximately 17° during the process of diving and -19° during the process of surfacing. A positive pitch angle indicates that the glider platform is heading down, and a negative pitch angle indicates that the glider platform is heading up.

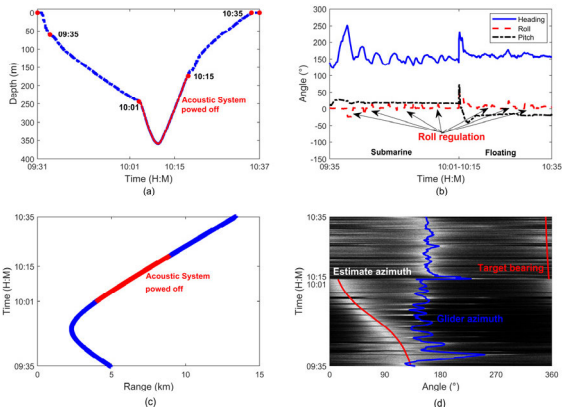

FIGURE 9. Experimental results in May 2018. (a) The change of the glider platform depth with time; (b) the change of the glider platform attitude angle with time; (c) the relative distance between the underwater glider and the experimental ship with time; (d) the estimation bearing recording pseudo-color graphic of the noise signal.

Fig. 9(c) gives the relative distance of the underwater glider and the experimental ship within the period of 09:35 to 10:35. Fig. 9(d) shows the estimation bearing pseudo-color graphic of the noise signal recorded by the acoustic system of underwater glider within the period of 09:35 to 10:35, among which the acoustic system is in power outage and stops working from 10:01-10:15. It can be seen from Fig. 9(c) and (d) that, in addition to receiving the noise signal of the experimental ship, the glider acoustic system is also interfered by the intermittent brake noise of itself within the period of 09:35-10:01. However, since the experimental ship is far away from the glider platform, the acoustic system mainly receives the noise signal which is produced by the glider platform within the period of 10:15 to 10:35. The direction of the connection line between the glider platform and the vector hydrophone relative to the true north is the estimation bearing of the noise signal, and also the glider output heading angle. With the interference of the intermittent brake noise of the glider platform, the farthest detection distance of the underwater glider to the experimental ship is only approximately 5 km. Thus, the interference has a

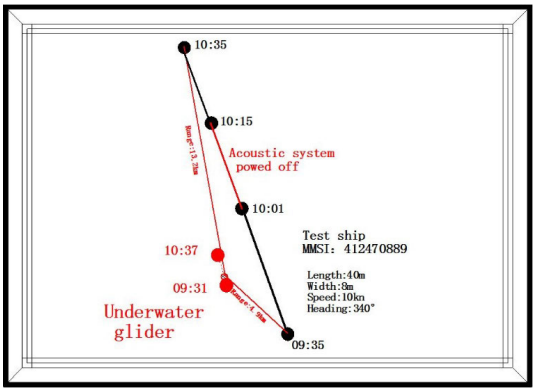

FIGURE 10. The detailed situation of the underwater glider and the experimental ship in May 2018.

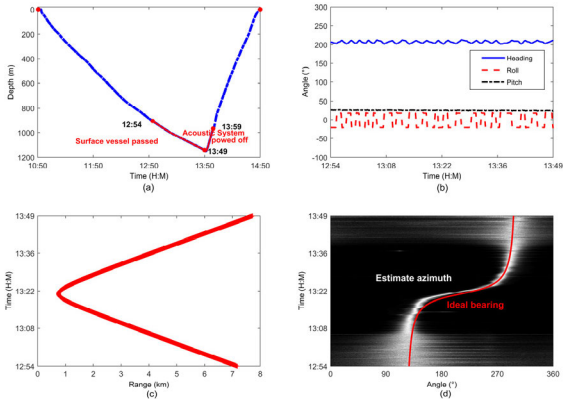

FIGURE 11. The experimental results in August, 2019. (a) The change of the glider platform depth with time; (b)the change of the glider platform attitude angle with time; (c) the relative distance between the glider platform and the experimental ship with time; (d) the estimation bearing recording pseudo-color graphic of the noise signal.

serious impact on the target detection performance of the glider acoustic system. Fig. 10 shows the detailed situation of the underwater glider and experimental ship within the period of 09:35 to 10:35. During the experiment, the velocity of the experimental ship is 10 kn and the heading direction is 340°. The underwater glider moves 1.8 km along with the direction of 343° at a speed of 1.0 kn.

C. EXPERIMENT ORGANIZED IN AUGUST of 2019

In response to the intermittent electromagnetic brake noise problem exposed in the experiment of May of 2018, the heading regulating mechanism was processed with the vibration and noise reduction, and meanwhile, the control strategy of the heading regulating mechanism was also optimized. In August of 2019, the experiment of vibration and noise reduction for the underwater glider platform was carried out in the South China Sea. The maximum diving depth of the glider was set to 1200 m during the experiment. Fig. 11 (a) shows the change of the platform depth with time during the working period of profile gliding. It can be seen that the maximum diving depth of the glider platform is 1152 m and a single profile takes about 4h. Within the period of 12:54 to 13:49, a surface ship (MMSI 414350640, 42 m in length and 6 m in width) passes near the glider platform, during which the glider dives from 905 m to 1042 m. Then, the acoustic system shuts down for 11 min during the glider drains oil to adjust its attitude and the buoyancy period (from 13:49 to 13:59). Fig. 11 (b) shows the change of the glider attitude angle with time. It can be seen that, during 12:54 to 13:49, the glider moves downwards with the pitch angle of 25° which remains approximately constant, but the heading angle and the roll angle change all the time to control the motion state. The change amplitude of the roll angle has been greatly improved compared with that before the vibration and noise reduction of the platform, which means that the heading regulating mechanism has better heading regulating capability. The amplitude change of the heading angle is approximately 8°, which has been improved greatly compared with that before the platform optimization too.

Fig. 11(c) gives the relative distance of the underwater glider and the experimental ship within the period of 12:54 to 13:49. The position of the experimental ship is obtained by the shipborne automatic identification system (AIS) receiver. Fig. 11(d) shows the estimation bearing pseudo-color graphic of the noise signal recorded by the acoustic system of underwater glider during the period of 12:54 to 13:49. It can be seen from Fig. 11(c) and (d) that the nearest distance between the glider platform and the experimental ship is 0.7 km, and the farthest distance is 7.7 km within the period of 12:54 and 13:49. During the entire experiment, the acoustic system of the glider detects and tracks the experimental ship without the interference of platform intermittent noise. However, since the underwater position of the glider platform obtained by interpolation is not accurate, there is a certain deviation between the target estimation bearing and the true bearing.

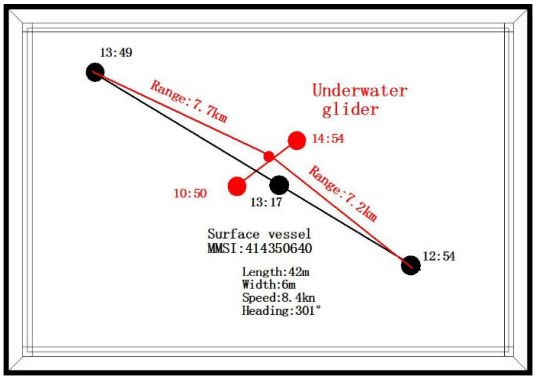

FIGURE 12. The detailed situation of the underwater glider and the experiment ship in August,2019.

Fig. 12 shows the detailed situation of underwater glider and the experimental ship during the period of 12:54 to 13:49. During the experiment, the experimental ship is kept at a speed of 8.4 kn and the heading direction is kept at 301°. The glider platform moves 3.0 km along with the direction

of 54°, and the gliding velocity is about 0.4 kn during the whole gliding period.

VI. CONCLUSION

In this study, the underwater glider platform is integrated with a single vector hydrophone, which develops a new type of underwater glider with target detection capability. Main noise sources of the glider platform are analyzed. According to noise production, transmission and interference mechanism, the glider is optimized for vibration and noise reduction from four aspects: the intensity reduction of the vibration source, the vibration frequency design of the heading regulating mechanism, blocking the transmission route of the noise, and the optimization design of the electromagnetic compatibility. Verified by the experiments, the results show that the noise interference of the optimized glider platform on the vector hydrophone is significantly reduced. The vector hydrophone acoustic pressure channel has the maximum noise reduction of 25 dB at 2 kHz frequency, but vector channels have the maximum noise reduction of 28 dB at 80 Hz frequency. The results of the two experiments organized in the South China Sea in May, 2018 and August, 2019 show that the farthest detection distance of the underwater glider to the surface ship with a speed of 10 kn is only approximately 5 km before the vibration and noise reduction of the glider platform, and the intermittent brake noise interference of the glider platform has a great influence on the vector hydrophone. After optimization, the farthest detection distance of the underwater glider to the surface ship with a speed of 8.4 kn reaches to 7.7 km and without the influence of the intermittent brake noise interference from the glider platform. The research will promote the application of the underwater unmanned platform on the target detection.

ACKNOWLEDGMENT

The authors thank the staff involved in the underwater glider experiments in the South China Sea in May of 2018 and August of 2019.

REFERENCES

[1] T. Curtin and E. Belcher, "Innovation in oceanographic instrumentation," *Oceanography*, vol. 21, no. 3, pp. 44–53, Sep. 2008.
[2] A. Alvarez, A. Caffaz, A. Caiti, G. Casalino, L. Gualdesi, A. Turetta, and R. Viviani, "Folaga: A low-cost autonomous underwater vehicle combining glider and AUV capabilities," *Ocean Eng.*, vol. 36, no. 1, pp. 24–38, Jan. 2009.
[3] L. Fang, W. Yan-Hui, and W. Shu-Xin, "Development of the hybrid underwater glider Petrel-II," *Sea Technol.*, vol. 55, no. 4, pp. 51–54, 2014.
[4] R. Damus, J. Manley, S. Desset, J. Morash, and C. Chryssostomidis, "Design of an inspection class autonomous underwater vehicle," in *Proc. Oceans MTS/IEEE*, Oct. 2002, pp. 180–185.
[5] C. Herve, B. Laurent, and P. Patrice, "Seaexplorer glider breaks two world records multisensor UUV achieves global milestones for endurance, distance," *Sea Technol.*, vol. 55, no. 3, pp. 19–22, 2014.
[6] Y. Jian-Cheng, L. Shi-Jie, and J. Wenming, "The present state of deep-sea underwater glider technologies and applications," *J. Eng. Stud.*, vol. 8, no. 2, pp. 208–216, 2016.
[7] S. Xin-Rui, W. Yan-Hui, and Y. Shao-Qiong, "Development of underwater gliders: An overview and prospect," *J. Unmanned Undersea Syst.*, vol. 26, no. 2, pp. 89–106, 2018.
[8] L. Lu and X. Ling, "Measurement and analysis of self-noise in hybrid-driven underwater gliders," *Chin. J. Ship Res.*, vol. 12, no. 4, pp. 132–139, 2017.
[9] L. Lu, X. Ling, and L. Shi-Quan, "Using Petrel II glider to analyze underwater noise spectrogram in the South China Sea," *Acoustic Aust.*, vol. 46, no. 2, pp. 1–8, 2018.
[10] M.-E. Fernández-García, J. Larrey-Ruiz, and J.-L. Sancho-Gómez, "Reducing the noise introduced by the engine of a moving autonomous vehicle for recording underwater sounds," *Appl. Acoust.*, vol. 155, pp. 250–259, Dec. 2019.
[11] J. D. Holmes, W. M. Carey, J. F. Lynch, A. E. Newhall, and A. Kukulya, "An autonomous underwater vehicle towed array for ocean acoustic measurements and inversions," *Eur. Oceans*, vol. 2, pp. 1058–1061, Jun. 2005.
[12] H. Matsumoto, J. H. Haxel, and R. P. Dziak, "Mapping the sound field of an erupting submarine volcano using an acoustic glider," *J. Acoust. Soc. Amer.*, vol. 129, no. 3, pp. 94–99, 2011.
[13] B. G. Ferguson, K. W. Lo, and J. D. Rodgers, "Sensing the underwater acoustic environment with a single hydrophone onboard an undersea glider," in *Proc. OCEANS IEEE Sydney*, May 2010, pp. 1–5.
[14] Y. Min-Jiang and J. Osler, "Underwater source localization using a hydrophone-equipped glider," *J. Acoust. Soc. Amer.*, vol. 19, pp. 1–5, Jun. 2013.
[15] J. Cheng, L. Jian-Long, and X. Wen, "The use of underwater gliders as acoustic sensing platforms," *Appl. Acoustic*, vol. 9, pp. 4839–4852, 2019.
[16] A. Gunes and M. B. Guldogan, "Joint underwater target detection and tracking with the Bernoulli filter using an acoustic vector sensor," *Digit. Signal Process.*, vol. 48, pp. 246–258, Jan. 2016.
[17] X.-H. Wang, J.-F. Chen, J. Han, and Y.-M. Jiao, "Optimization for the direction of arrival estimation based on single acoustic pressure gradient vector sensor," *Int. J. Nav. Archit. Ocean Eng.*, vol. 6, no. 1, pp. 74–86, Mar. 2014.
[18] S. Najeem, K. Kiran, A. Malarkodi, and G. Latha, "Open lake experiment for direction of arrival estimation using acoustic vector sensor array," *Appl. Acoust.*, vol. 119, pp. 94–100, Apr. 2017.
[19] M. Aktas and H. Ozkan, "Acoustic direction finding using single acoustic vector sensor under high reverberation," *Digit. Signal Process.*, vol. 75, pp. 56–70, Apr. 2018.
[20] Z. Liang-ming, *Research on Properties and Applications of Vector Acoustic Field in Shallow Water Vector Hydrophone*. Beijing, China: Chinese Academy of Sciences, 2015.
[21] S. Qin-Dong, D. Liang-Long, and H. Wen-Shu, "Design of a new real-time gesture correction vector hydrophones," *Tech. Acoust.*, vol. 34, no. 2, pp. 304–307, 2015.
[22] S. Qin-Dong, H. Wen-Shu, and W. Wen-Long, "The design and implementation for three dimension co-vibrating vector hydrophone," *Chin. J. Sens. Actuators*, vol. 29, no. 6, pp. 952–956, 2016.
[23] A. R. Barnard and S. A. Hambric, "Design and implementation of a shielded underwater vector sensor for laboratory environments," *J. Acoust. Soc. Amer.*, vol. 130, no. 6, pp. 386–391, 2011.

CHAO WANG received the B.Sc. degree from Harbin Engineering University in 2010 and the M.Sc. and Ph.D. degrees from the Navy Submarine Academy in 2013 and 2017, respectively. He is currently an Assistant Researcher with the Navy Submarine Academy. His main research interests focus on ocean ambient noise and acoustic signal processing.

MENG YUAN received the B.Sc. degree from Lanzhou University in 2016 and the M.Sc. degree from the National University of Defense Technology in 2018. He is currently pursuing the Ph.D. degree with the Navy Submarine Academy. His main research interests focus on pattern recognition and acoustic signal processing.